

Carbonate Regeneration Using a Membrane Electrochemical Cell for Efficient CO₂ Capture

Alexander P. Muroyama* and Lorenz Gubler

Cite This: *ACS Sustainable Chem. Eng.* 2022, 10, 16113–16117

Read Online

ACCESS |



Metrics & More



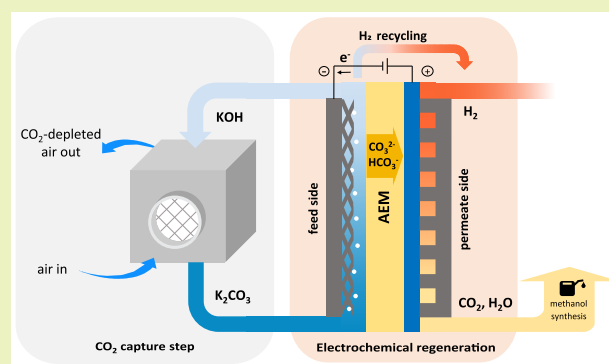
Article Recommendations



Supporting Information

ABSTRACT: The use of atmospheric CO₂ as a chemical feedstock is a promising way to decarbonize the chemical and transportation sectors, which currently rely heavily on fossil fuels. This transition demands new technologies to reduce the energy required to capture and separate CO₂. Here, we develop and demonstrate an alternative method of carbonate solution regeneration using an anion exchange membrane electrochemical cell. This process simultaneously regenerates the CO₂ capture solution on the feed side, while enriching a stream of H₂ with CO₂ on the permeate side of the cell. Preliminary results show a CO₂ transport faradaic efficiency of 50% (100% CO₃²⁻ transport) when supplying a pure K₂CO₃ solution at current densities up to 60 mA·cm⁻². A small cathode gap benefited cell operation by preventing membrane transport of OH⁻, although with an increased ohmic resistance. This represents a step forward in the application of electrochemistry to drive processes that are critical to CO₂ valorization.

KEYWORDS: CO₂ capture, direct air capture, anion exchange membrane, alkaline electrochemistry, carbonate, electrochemical regeneration



INTRODUCTION

The massive scale of global anthropogenic CO₂ emissions and the ever-increasing concentration of atmospheric CO₂ necessitate a coordinated and multifaceted approach toward decarbonization to avoid catastrophic climate change.¹ This will need to take place through, among other efforts, a phase-out of fossil fuels, increased deployment of renewable energy, and widespread carbon capture and utilization/sequestration for hard-to-decarbonize sectors. Electrochemical methods of CO₂ capture represent a promising alternative to conventional thermally driven capture processes, as they can efficiently utilize cheap renewable electrons and have flexible architectures for plug-and-play integration.^{2–4} These approaches could also be readily coupled with electrochemical valorization processes (e.g., electrolysis) to provide chemicals or liquid fuels.⁵

In order to have a closed carbon cycle, CO₂ captured for combustible synfuels must have a nonfossil origin. It will not be technologically feasible, for example, to incorporate onboard CO₂ capture for commercial aviation in the near term. Therefore, direct-air capture (DAC) is a preferred technological route for a CO₂-to-products scenario.^{6,7} Because of the relatively minute quantity of CO₂ contained in air, this presents technical challenges associated with processing large amounts of air and efficiently running an electrochemical process to remove it. Previous work has shown that direct gas phase separation of CO₂ from air is possible using an electrochemical cell, but faradaic

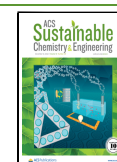
efficiencies and current densities are inherently limited by the flow of reactants.^{8,9} The incorporation of an inexpensive capture solution (e.g., KOH, NaOH) addresses this challenge, as much higher current densities can be applied to regenerate a solution that contains CO₂ in a concentrated form (e.g., carbonate, bicarbonate).

The most mature technology for electrochemical CO₂ regeneration from carbonate is bipolar membrane electrodialysis (BPMED).^{10–12} Previous studies have investigated the use of an ion-exchange membrane stack to regenerate carbonate capture solutions with current densities exceeding 100 mA·cm⁻².^{13,14} The key challenges associated with this approach are large ohmic resistances in the stack, undesirable reactions at the electrodes, and resistances due to gas evolution within the stack,^{12,13} in addition to the relatively high cost of bipolar membranes.¹⁰ Another approach that has been explored is a three compartment cell containing two cation exchange membranes, employing a H₂-depolarized anode to release CO₂ from a carbonate solution.¹⁵ This approach has achieved an experimental energy

Received: July 12, 2022

Revised: October 18, 2022

Published: November 28, 2022



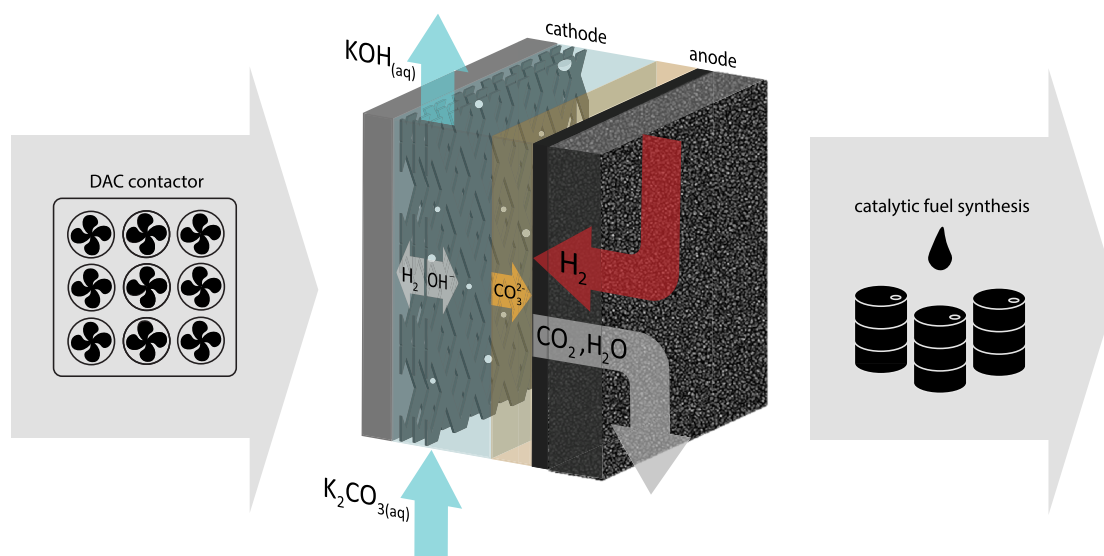
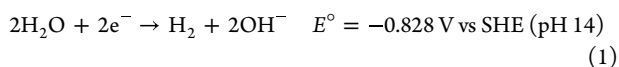


Figure 1. Schematic of the electrochemical regeneration process (dimensions not to scale).

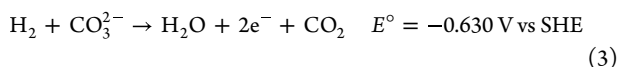
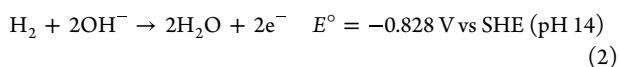
consumption of $374 \text{ kJ} \cdot \text{mol}_{\text{CO}_2}^{-1}$ at a current density of $5 \text{ mA} \cdot \text{cm}^{-2}$. Other studies have investigated the direct electrochemical conversion of carbonate solution¹⁶ to form CO^{17–21} or formate.²² These systems utilize a bipolar membrane to dissociate H₂O and generate protons to drive acid–base reactions with (bi)carbonate. As a result, significant amounts of H₂ are generated at overpotentials that are high compared to state-of-the-art proton exchange membrane water electrolysis.²³ There is therefore a need to explore alternative regeneration approaches that have the potential to reduce overall energy requirements while providing flexibility in the molar ratios of CO₂:H₂ produced.

EXPERIMENTAL SECTION

We propose a new method of CO₂ regeneration from a carbonate capture solution (K₂CO₃) through a driven anion exchange membrane (AEM) cell depolarized with hydrogen. This design overcomes the limitations in efficiency and current density that arise in direct gas phase separation of <1% concentration CO₂ using AEMs.⁸ The relevant electrochemical reactions are the hydrogen evolution reaction (HER) on the cathode side, taking place in the aqueous capture solution:



and the hydrogen oxidation reaction (HOR) in the presence of carbonate on the anode side, taking place in the gas phase:



According to the above equations, there is no net consumption or generation of H₂ in the system. However, there is the possibility that small amounts of dissolved O₂ from the capture step will be present in the solution, leading to a minimal rate of the oxygen reduction reaction (ORR) at the cathode. Given air contacting, the dissolved concentration of O₂ at 25 °C will be $0.24 \text{ mmol} \cdot \text{L}^{-1}$, and even lower in the presence of a dissolved salt.²⁴ At a solution flow rate of $5 \text{ mL} \cdot \text{min}^{-1}$, for example, this yields a maximum ORR current density of $0.8 \text{ mA} \cdot \text{cm}^{-2}$, assuming that all of the O₂ is consumed. Thus, the dominant cathode reaction will still be the HER rather than the ORR. The evolved H₂ separated from the cathode loop can be recycled to the anode side, and KOH exiting the cell can be recycled to the capture step. External

H₂ would need to be provided to reach appropriate ratios of H₂:CO₂ for downstream fuel synthesis. The benefit of depolarizing the cell with H₂ is the reduction of overpotentials across the cell and the relative ease of H₂O separation from the product stream compared with O₂. The process is shown schematically in Figure 1. The net result is the extraction of CO₂ from the carbonate solution on the anode (= permeate) side and an aqueous solution with a higher pH exiting the cell on the cathode (= feed) side, and the resulting mixture of CO₂ and residual H₂ could be used for catalytic fuel synthesis such as methanol (MeOH) synthesis.^{25–27} Direct electrochemical conversion of CO₂ to MeOH is an area of ongoing research that is still in an early stage compared to thermocatalytic approaches due to challenges with catalyst selectivity, activity, and stability.²⁸

We performed a series of galvanostatic experiments using a cell with an active area of 10 cm^2 , the details of which can be found in the Supporting Information. A stainless steel expanded mesh served as the cathode and a Pt/C catalyst-coated gas diffusion electrode as the anode, and the two compartments were separated by an AEM. Two different gap distances between the cathode and membrane, a zero gap and a 1 mm gap, were achieved by using different thicknesses of a PTFE flow frame. An additional PP mesh was used in the 1 mm gap to support the membrane on the cathode side. In all experiments, reactions on the cathode took place in the liquid phase, and reactions on the anode took place in the gas phase at ambient temperatures and pressures. No external humidification of gases was necessary, as sufficient H₂O was produced on the anode through hydrogen oxidation and electro-osmotic drag from the cathode to the anode. A K₂CO₃ solution was fed to the cathode at $5 \text{ mL} \cdot \text{min}^{-1}$ using a peristaltic pump, and cell voltage, anode-side CO₂ concentration, and cathode pH were temporally monitored. The key performance metrics that follow from the data are faradaic efficiency and molar specific energy consumption. Due to the detection limit of the gas analysis, specific ratios of H₂:CO₂ were not targeted, but this could feasibly be accomplished through adjustment of the H₂ flow and/or operating current density.

RESULTS AND DISCUSSION

The cathode gap width plays a critical role in the transport of CO₃²⁻ to the membrane and OH⁻ out of the cell, as shown schematically in Figure 2. The zero-gap electrode configuration is commonly used in alkaline water electrolysis to reduce the ohmic losses.²⁹ However, unlike in alkaline electrolysis, the present system has the additional challenge of maximizing transport of CO₃²⁻ from the incoming solution across the membrane. For this reason, a zero-gap configuration has

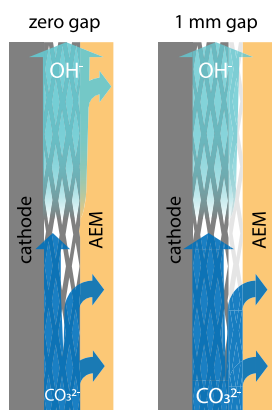


Figure 2. Schematic demonstrating the effect of gap width on ion transport within the cathode compartment. The 1 mm gap increases the ohmic drop but reduces the possibility of undesirable OH^- transport in the AEM. The zero-gap configuration decreases the ohmic drop but increases OH^- transport in the AEM.

competing effects: the ohmic drop decreases and OH^- generated at the cathode is more likely to be transported across the membrane instead of CO_3^{2-} . In addition, the gap width has an influence on bubble transport by affecting the velocity of the flow.

The results of cell polarizations with the two gap widths using 1 M K_2CO_3 as the catholyte are shown in Figure 3. The clear effect of the zero gap on ohmic drop is observed in Figure 3a, which shows the area specific resistance (ASR), determined using impedance spectroscopy, plotted against current density. The ASR of the zero-gap cell is approximately half of that of the 1 mm gap cell, indicating that the reduced gap width allows for more efficient ion conduction through a shorter path length and possibly enhanced bubble transport. The zero gap leads to a drop in the faradaic efficiency to $\sim 35\%$ at current densities $>20 \text{ mA}\cdot\text{cm}^{-2}$ (Figure 3b), indicating that significant amounts of OH^- generated at the cathode are transported across the AEM. These competing effects result in a larger energy consumption for the zero-gap configuration, as shown in Figure 3c. Therefore, the more critical influence is the undesired OH^- transport, and one essential goal of future electrode designs should be the optimization of CO_3^{2-} and OH^- flows within the system.

The results of the cell polarizations with varying carbonate solution molarity using the 1 mm gap configuration are presented in Figure 4. The full and iR -corrected cell voltages (Figure 4a) show an effect of the solution molarity on the ohmic resistance in the cell, particularly for the 0.5 M solution at higher current densities. The conductivities of the 0.5, 1, and 2 M solutions were measured to be 80, 144, and $217 \text{ mS}\cdot\text{cm}^{-1}$, respectively, and therefore, the lower concentration of solution induces a greater voltage drop. The faradaic efficiency (Figure 4b) is not significantly affected by solution molarity, although values are slightly higher for the higher molarity solution. Thus, CO_3^{2-} is the primary charge carrier in the system, corresponding to a faradaic efficiency of 50%, with some OH^- transport accounting for lower values and electro-osmotic drag accounting for slightly higher values (as in the case for the 2 M solution). In order for values significantly greater than 50% to be reached, HCO_3^- must be a charge carrier; however, this will require further exposure of the solution to atmospheric CO_2 and an associated increase in the energy expense of the capture step.^{13,16}

This aspect is further discussed in the Supporting Information. The differences in the process energy consumption (Figure 4c) can be mostly attributed to the effect of solution concentration on cell voltage. The 1 and 2 M solutions yield similar energy consumptions at the current densities tested, although the 2 M solution likely becomes advantageous at larger current densities due to the increased influence of ohmic losses. The 0.5 M solution generally has the highest energy consumption, with the minimum value occurring at $20 \text{ mA}\cdot\text{cm}^{-2}$ due to the steep increase in faradaic efficiency. While operating at high current densities is critical in reducing the capital expenditures of the regeneration step, there were challenges operating at higher current densities in the form of higher, less stable cell voltages. Further studies investigating the breakdown in cell overpotentials, pH change, effect of catholyte flow rate, and effect of KOH/KHCO_3 in the system are presented in the Supporting Information.

Within the landscape of CO_2 capture and conversion technologies, there are a number of different routes by which carbonate or bicarbonate can be electrochemically transformed into value-added products.¹⁶ The present approach occupies a unique position in the electrochemical CO_2 capture field, as it requires H_2 for operation, but conceptually does not result in any net consumption of H_2 if evolved H_2 is separated and recycled

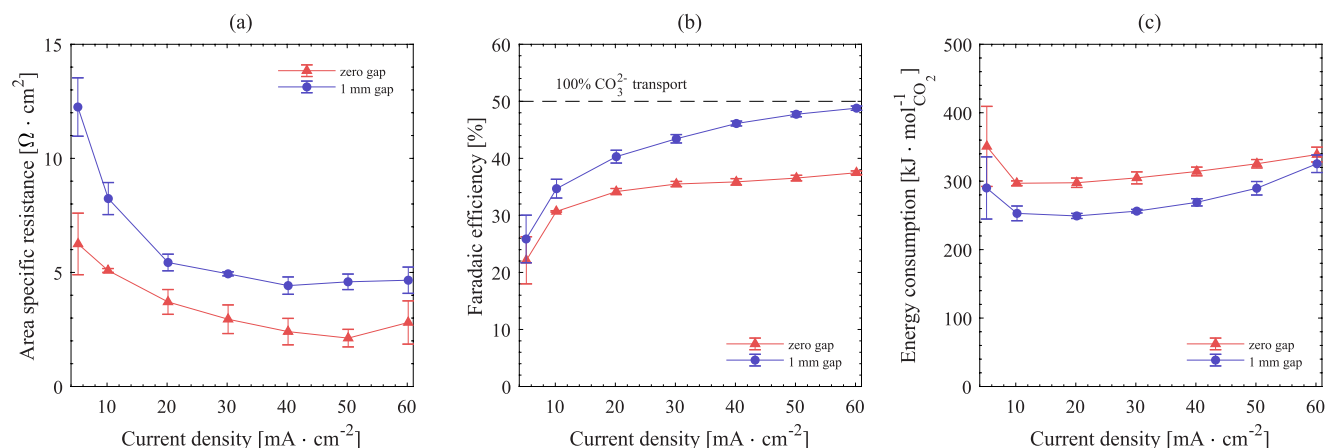


Figure 3. (a) Area specific resistance, (b) faradaic efficiency, and (c) energy consumption for a 1 M K_2CO_3 solution plotted against current density for the 1 mm gap and zero-gap cathode configurations. Error bars represent standard deviations for triplicate experiments.

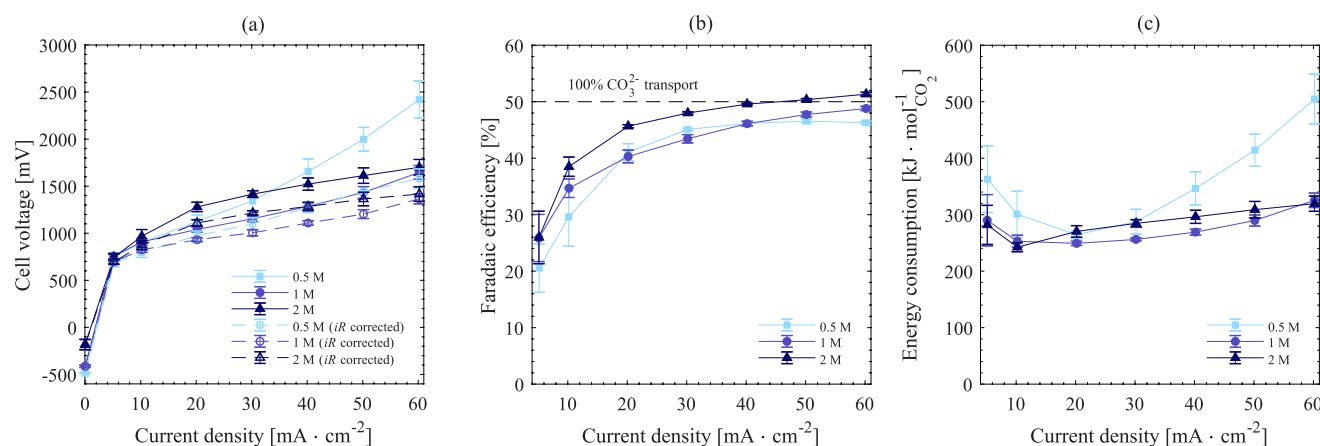


Figure 4. (a) Uncorrected and *iR*-corrected cell voltage, (b) faradaic efficiency, and (c) energy consumption for the 0.5, 1, and 2 M solutions of K₂CO₃ plotted against current density. Error bars represent standard deviations for triplicate experiments.

from the cathode to the anode. In addition, by avoiding CO₂ conversion, lower potentials are required to drive a more selective process. The ratio of H₂:CO₂ could therefore be tuned by changing the flow rate of H₂ on the anode side of the cell such that it is suitable for a downstream catalytic process, for example, 3 for MeOH synthesis or 4 for synthetic natural gas (Sabatier process). A separate PEM electrolysis process could provide the H₂ at high efficiencies and current densities, and the described electrochemical carbonate process could be used to subsequently “enrich” the stream with atmospheric CO₂. There could be additional benefits to the proposed approach, such as the ability to operate the cell at increased pressures and enrich a pressurized H₂ stream while suppressing bubble formation at the cathode and reducing losses. A continuously pressurized process would not be possible in a BPMED configuration, for example, as the system needs to be depressurized in order to liberate the dissolved CO₂ from the solution.¹⁴ The present system compares favorably with BPMED in terms of energy consumption¹³ while addressing some of the previously stated issues with that approach.

The development of novel electrochemical conversion methodologies necessitates a discussion on how they could be integrated with conventional, scaled technologies. A conservative estimate for the required energy for water electrolysis is 400 kJ · mol⁻¹ (60% LHV efficiency),^{25,30} and 3 mol are required for every 1 mol of CO₂ for the synthesis of methanol. Therefore, the water electrolysis process would require 1200 kJ · mol⁻¹ MeOH. As the CO₂ capture step is thermodynamically downhill, it has a relatively low energy consumption of 13–30 kJ · mol⁻¹ CO₂ for fan and pumping requirements in the air contactor.^{31,32} The next critical piece is the electrochemical CO₂ enrichment process, which could have energy requirements between 200 and 300 kJ · mol⁻¹ CO₂. The MeOH synthesis step (i.e., CO₂ hydrogenation) will also require energy, but is a commercially mature process^{26,27} (TRL 7) with recent plants producing MeOH at the 100 kton per annum scale.³³ The reaction itself is exothermic, but an integrated plant would require an estimated 169 kJ · mol⁻¹ MeOH of energy due to compression, pumping, and auxiliary heating and cooling requirements, according to modeling performed for a commercial scale plant.²⁷ This brief analysis does not represent a full accounting of energy requirements for every plant component, but provides a rough estimate of 1582–1699 kJ · mol⁻¹ MeOH for the entire process, making it between 43% and 46% efficient in terms of HHV_{MeOH}

(727 kJ · mol⁻¹ MeOH). For reference, an analysis of a methanol plant based on steam methane reforming found an equivalent energy input of 1070 kJ · mol⁻¹ MeOH, or an overall efficiency of 68%.³⁴ It should be noted, however, that starting from a fossil fuel provides a thermodynamic advantage over air as the feedstock and leads to a significantly higher greenhouse gas contribution over the life cycle of the fuel.

CONCLUSIONS

We have proposed and tested an electrochemical process that utilizes an AEM to enrich an H₂ stream with CO₂ originating from a carbonate capture solution. Initial results show a stable operation and a clear electrochemical carbonate pumping effect from the solution, with the carbonate concentration and electrode gap width influencing performance. Minimum energy consumption was 240 kJ · mol⁻¹ CO₂. In order to develop the electrochemical CO₂ enrichment concept further, overpotentials should be reduced through judicious catalyst selection and electrode design. In addition, efforts should be made to improve the industrial relevance of the application by increasing the current density, duration, and possibly the pressure of cell operation. A deeper understanding of the implications of the coupled air capture process (e.g., (bi)carbonate ion concentrations vs mode and duration of air contact, optimal solution concentrations) would benefit the field of (bi)carbonate electrochemistry as well. These advancements will allow CO₂ capture and utilization routes to become less energy and cost intensive and therefore open pathways for scaled deployment.

ASSOCIATED CONTENT

Supporting Information

The Supporting Information is available free of charge at <https://pubs.acs.org/doi/10.1021/acssuschemeng.2c04175>.

Experimental methods, breakdown in cell overpotentials, pH changes, faradaic efficiency as a function of catholyte flow rate, and influence of the extent of carbonation in the solution (PDF)

AUTHOR INFORMATION

Corresponding Author

Alexander P. Muroyama – Electrochemistry Laboratory, Paul Scherrer Institut, 5232 Villigen PSI, Switzerland;

orcid.org/0000-0003-1535-8032;

Email: alexander.muroyama@psi.ch

Author

Lorenz Gubler – Electrochemistry Laboratory, Paul Scherrer Institut, 5232 Villigen PSI, Switzerland; orcid.org/0000-0002-8338-6994

Complete contact information is available at:

<https://pubs.acs.org/10.1021/acssuschemeng.2c04175>

Notes

The authors declare no competing financial interest.

ACKNOWLEDGMENTS

The authors wish to thank the Swiss National Science Foundation (SNSF) for project funding (Grant No. 201881). The authors would also like to thank Dino Aegerter and Simon Leisibach for assistance in implementation of the reference electrode.

REFERENCES

- (1) Masson-Delmotte, V.; Zhai, P.; Pirani, A.; Connors, S. L.; Péan, C.; Berger, S.; Caud, N.; Chen, Y.; Goldfarb, L.; Gomis, M. I. *Climate Change 2021: The Physical Science Basis*; IPCC, 2021.
- (2) Muroyama, A.; Pătru, A.; Gubler, L. Review—CO₂ Separation and Transport via Electrochemical Methods. *J. Electrochem. Soc.* **2020**, *167* (13), 133504.
- (3) Sharifian, R.; Wagterveld, R. M.; Digdaya, I. A.; Xiang, C.; Vermaas, D. A. Electrochemical carbon dioxide capture to close the carbon cycle. *Energy Environ. Sci.* **2021**, *14* (2), 781–814.
- (4) Shaw, R. A.; Hatton, T. A. Electrochemical CO₂ capture thermodynamics. *International Journal of Greenhouse Gas Control* **2020**, *95*, 102878.
- (5) van Bavel, S.; Verma, S.; Negro, E.; Bracht, M. Integrating CO₂ Electrolysis into the Gas-to-Liquids-Power-to-Liquids Process. *ACS Energy Lett.* **2020**, *5* (8), 2597–2601.
- (6) Keith, D. W. Why Capture CO₂ from the Atmosphere? *Science* **2009**, *325* (5948), 1654–1655.
- (7) Sanz-Pérez, E. S.; Murdock, C. R.; Didas, S. A.; Jones, C. W. Direct Capture of CO₂ from Ambient Air. *Chem. Rev.* **2016**, *116* (19), 11840–11876.
- (8) Muroyama, A. P.; Beard, A.; Pribyl-Kranewitter, B.; Gubler, L. Separation of CO₂ from Dilute Gas Streams Using a Membrane Electrochemical Cell. *ACS ES&T Engineering* **2021**, *1* (5), 905–916.
- (9) Eisaman, M.; Schwartz, D.; Amic, S.; Larner, D.; Zesch, J.; Torres, F.; Littau, K. Energy-efficient electrochemical CO₂ capture from the atmosphere. In *Technical Proceedings of the 2009 Clean Technology Conference and Trade Show*; Citeseer, 2009; pp 3–7.
- (10) Sabatino, F.; Mehta, M.; Grimm, A.; Gazzani, M.; Gallucci, F.; Kramer, G. J.; van Sint Annaland, M. Evaluation of a Direct Air Capture Process Combining Wet Scrubbing and Bipolar Membrane Electrodialysis. *Ind. Eng. Chem. Res.* **2020**, *59* (15), 7007–7020.
- (11) Iizuka, A.; Hashimoto, K.; Nagasawa, H.; Kumagai, K.; Yanagisawa, Y.; Yamasaki, A. Carbon dioxide recovery from carbonate solutions using bipolar membrane electrodialysis. *Sep. Purif. Technol.* **2012**, *101*, 49–59.
- (12) Nagasawa, H.; Yamasaki, A.; Iizuka, A.; Kumagai, K.; Yanagisawa, Y. A new recovery process of carbon dioxide from alkaline carbonate solution via electrodialysis. *AIChE J.* **2009**, *55* (12), 3286–3293.
- (13) Eisaman, M. D.; Alvarado, L.; Larner, D.; Wang, P.; Garg, B.; Littau, K. A. CO₂ separation using bipolar membrane electrodialysis. *Energy Environ. Sci.* **2011**, *4* (4), 1319–1328.
- (14) Eisaman, M. D.; Alvarado, L.; Larner, D.; Wang, P.; Littau, K. A. CO₂ desorption using high-pressure bipolar membrane electrodialysis. *Energy Environ. Sci.* **2011**, *4* (10), 4031–4037.
- (15) Shu, Q.; Legrand, L.; Kuntke, P.; Tedesco, M.; Hamelers, H. V. M. Electrochemical Regeneration of Spent Alkaline Absorbent from Direct Air Capture. *Environ. Sci. Technol.* **2020**, *54* (14), 8990–8998.
- (16) Welch, A. J.; Dunn, E.; DuChene, J. S.; Atwater, H. A. Bicarbonate or Carbonate Processes for Coupling Carbon Dioxide Capture and Electrochemical Conversion. *ACS Energy Lett.* **2020**, *5* (3), 940–945.
- (17) Li, T.; Lees, E. W.; Goldman, M.; Salvatore, D. A.; Weekes, D. M.; Berlinguette, C. P. Electrolytic Conversion of Bicarbonate into CO in a Flow Cell. *Joule* **2019**, *3* (6), 1487–1497.
- (18) Li, Y. C.; Lee, G.; Yuan, T.; Wang, Y.; Nam, D.-H.; Wang, Z.; García de Arquer, F. P.; Lum, Y.; Dinh, C.-T.; Voznyy, O.; et al. CO₂ Electroreduction from Carbonate Electrolyte. *ACS Energy Lett.* **2019**, *4* (6), 1427–1431.
- (19) Lees, E. W.; Goldman, M.; Fink, A. G.; Dvorak, D. J.; Salvatore, D. A.; Zhang, Z.; Loo, N. W. X.; Berlinguette, C. P. Electrodes Designed for Converting Bicarbonate into CO. *ACS Energy Lett.* **2020**, *5* (7), 2165–2173.
- (20) Zhang, Z.; Lees, E. W.; Habibzadeh, F.; Salvatore, D. A.; Ren, S.; Simpson, G. L.; Wheeler, D. G.; Liu, A.; Berlinguette, C. P. Porous metal electrodes enable efficient electrolysis of carbon capture solutions. *Energy Environ. Sci.* **2022**, *15* (2), 705–713.
- (21) Kim, Y.; Lees, E. W.; Berlinguette, C. P. Permeability Matters When Reducing CO₂ in an Electrochemical Flow Cell. *ACS Energy Lett.* **2022**, *7*, 2382–2387.
- (22) Li, T.; Lees, E. W.; Zhang, Z.; Berlinguette, C. P. Conversion of Bicarbonate to Formate in an Electrochemical Flow Reactor. *ACS Energy Lett.* **2020**, *5* (8), 2624–2630.
- (23) Ayers, K. High efficiency PEM water electrolysis: enabled by advanced catalysts, membranes, and processes. *Current Opinion in Chemical Engineering* **2021**, *33*, 100719.
- (24) Millero, F. J.; Huang, F.; Laferriere, A. L. Solubility of oxygen in the major sea salts as a function of concentration and temperature. *Mar. Chem.* **2002**, *78* (4), 217–230.
- (25) Kauw, M.; Benders, R. M. J.; Visser, C. Green methanol from hydrogen and carbon dioxide using geothermal energy and/or hydropower in Iceland or excess renewable electricity in Germany. *Energy* **2015**, *90*, 208–217.
- (26) Marlin, D. S.; Sarron, E.; Sigurbjörnsson, Ó. Process Advantages of Direct CO₂ to Methanol Synthesis. *Frontiers in Chemistry* **2018**, *6*, 446.
- (27) Pérez-Fortes, M.; Schöneberger, J. C.; Boulamanti, A.; Tzimas, E. Methanol synthesis using captured CO₂ as raw material: Techno-economic and environmental assessment. *Applied Energy* **2016**, *161*, 718–732.
- (28) Albo, J.; Alvarez-Guerra, M.; Castaño, P.; Irabien, A. Towards the electrochemical conversion of carbon dioxide into methanol. *Green Chem.* **2015**, *17* (4), 2304–2324.
- (29) Haverkort, J. W.; Rajaei, H. Voltage losses in zero-gap alkaline water electrolysis. *J. Power Sources* **2021**, *497*, 229864.
- (30) Smith, W. A.; Burdyny, T.; Vermaas, D. A.; Geerlings, H. Pathways to Industrial-Scale Fuel Out of Thin Air from CO₂ Electrolysis. *Joule* **2019**, *3* (8), 1822–1834.
- (31) Baciocchi, R.; Storti, G.; Mazzotti, M. Process design and energy requirements for the capture of carbon dioxide from air. *Chem. Eng. Process.* **2006**, *45* (12), 1047–1058.
- (32) Keith, D. W.; Holmes, G.; St. Angelo, D.; Heidel, K. A Process for Capturing CO₂ from the Atmosphere. *Joule* **2018**, *2* (8), 1573–1594.
- (33) Carbon Recycling International. <https://www.carbonrecycling.is/> (accessed Sept. 27, 2021).
- (34) Milani, D.; Khalilpour, R.; Zahedi, G.; Abbas, A. A model-based analysis of CO₂ utilization in methanol synthesis plant. *J. CO₂ Util.* **2015**, *10*, 12–22.